Phys. Status Solidi A **208**, No. 1, 210–214 (2011) / **DOI** 10.1002/pssa.201026183

physica status solidi a
www.pss-a.com
applications and materials science

Temperature dependence of dark current in a p–i–n photodiode incorporating a resonant tunneling structure

Azzouz Sellai[*,1], Mohamed Henini[2], and Zahir Ouennoughi[,1]**

[1] Physics Department, Sultan Qaboos University, P.O. Box 36, 123 Muscat, Oman
[2] School of Physics and Astronomy, Nottingham University, NG72RD, Nottingham, UK

Received 7 April 2010, revised 2 August 2010, accepted 4 August 2010
Published online 7 September 2010

Keywords dark current, electrical conduction, p–i–n diodes, photodiodes, resonant tunneling

[*] Corresponding author: e-mail asellai@squ.edu.om, Phone: +00 968 24141486, Fax: +00 968 24414228.
[**] On leave from Département de Physique, UFAS, Sétif, Algérie.

Analyses of the slope variations, as a function of temperature, of the dark current–voltage curves obtained in the case of p–i–n diodes incorporating in their intrinsic region a double barrier single quantum well (QW) structure indicate that below the flat band condition a conduction mechanism by tunneling assisted by recombination centers prevails over most of the temperature range considered (20–300 K). Above the flat band condition and for temperatures below 180 K, negative differential resistance (NDR) regions displaying Z-shaped bistability were observed. The appearance of these NDRs is attributed to resonant tunneling of holes via the lowest light-hole subband in the QW and electrons via the second quasi-bound level in the conduction band.

1 Introduction Besides revealing many interesting fundamental properties, p–i–n GaAs-based structures incorporating quantum wells (QWs) have been proposed and successfully used in a whole emerging class of enhanced functionality optoelectronic devices. These include light modulators, high-performance lasers, light-emitting diodes (LEDs), photodetectors, resonant tunneling devices as well as solar cells [1–9]. Their many advantages include high mobility, efficient and fast recombination rates, and the possibility to conveniently tailor the intrinsic region so as to optimize device parameters such as quantum efficiency and high speed of operation. GaAs p–i–n LEDs have also been recently used to demonstrate upconversion luminescence and/or electroluminescence, a mechanism in which it is possible to achieve emission of photons with energies in excess of what is supplied by an external source [10]. This process is of potential interest in many photonic devices. THz photomixers based on nano-pin diodes of much superior performance than conventional pin photomixers have too been developed lately [11]. In topical publications by Bavencove et al. [12] and Miki et al. [13], LEDs of nanometric scale incorporating multi-QWs have been fabricated and shown to exhibit dramatic improvement in light emission efficiency as well as extremely low dark leakage currents.

From the fundamental physics point of view, p–i–n, structures allow investigating transport due to both electrons and holes since it is possible, in principle, in a p–i–n structure to separate – depending on the applied bias – the contribution of electrons and holes to the conduction mechanism [1].

Moreover, it has been suggested and shown that notable improvements in the efficiency of light absorption and carrier transit times in the p–i–n structures could be achieved through the incorporation of single or multiple QWs in the intrinsic i-region.

In particular, it has been demonstrated both theoretically [2] and experimentally [3] that energy conversion efficiency (photocurrent) can be enhanced if QW and barrier systems are incorporated in the intrinsic region of p–i–n photodiodes or p–i–n solar cells. In detector structures the tunneling barrier is usually utilized for the purpose of blocking the dark current while permitting the flow of photocurrent due to resonance effects.

The insertion of a single or multiple QW(s) was shown, however, to affect the dark current in these p–i–n structures [4, 5]. Since the operation conditions of a p–i–n based photodetector depend on the dark properties of the device, understanding the dark electrical conduction mechanisms is, therefore, an important step in the task of improving devices efficiency. The variation of the dark current with temperature in the case of a bipolar resonant tunneling p–i–n diode is investigated in the present work, with the aim of clarifying possible charge transport phenomena that might prevail depending on the operating temperatures and applied bias.

2 Device structure and measurements The p–i–n diodes under investigation were grown on an n+ GaAs substrate by MBE as outlined in Ref. [1]. As Fig. 1 illustrates, the diodes consist of an n-doped GaAs layer, the intrinsic (i) region, followed by a top heavily doped p+ GaAs layer. The intrinsic region itself consists of a 6.2 nm thick undoped GaAs QW sandwiched between two 3 nm thick undoped AlAs barriers. A thin layer (1.8 ML) of self assembled InAs quantum dots (QDs) was also embedded in the GaAs well region. Undoped 60 and 100 nm spacer layers separate the doped contact regions from the double barrier structure to avoid diffusion of impurities into the QW during growth. Samples were processed as circular mesas of diameters 100–400 μm. Au/Ge/Ni alloys were used for top and bottom Ohmic contacts. The devices were initially designed to investigate the charging effects in tunneling transport through QWs and QDs.

The diodes were characterized by current–voltage (I–V) at different temperatures. The (I–V) measurements were conducted using a Keithley 2400 source-meter. The temperature control was attained using a Janis helium-closed-cycle refrigeration system with a Lakeshore 331 as the temperature controller. The investigation is done over a wide range of temperatures (20–300 K) with a measurement-accuracy better than 0.1 K.

3 Results and discussion The measured forward current over the temperature range considered show, to some extent, thermal activation with the I–V plots (Fig. 2) displaying different regions pertaining possibly to different conduction mechanisms.

The characteristics exhibit some noisy behavior particularly at lower temperatures, which is likely due to the limitations of the current measuring device since the current magnitude is well in the sub-nano Ampere region.

Various conduction mechanisms contributing to the current in a photodiode can be expressed by the general (I–V) equation:

$$I = I_s(T)\left(e^{qV/nkT} - 1\right). \tag{1}$$

It is generally the ideality factor (n) and the saturation current (I_s) and their dependence on temperature, in particular, that determine which conduction process prevails at which given temperature- and/or voltage-range.

For instance, n should be very close to unity for a purely diffusion current, while it should be equal to 2 in the case of generation-recombination via trap centers. A value of n comprised between 1 and 2 indicates usually the presence of both diffusion and recombination processes.

Also, considering the variations of n and I_s with temperature is one of the standard approaches to gain information on the relative contribution of tunneling in the measured dark current of a photodiode.

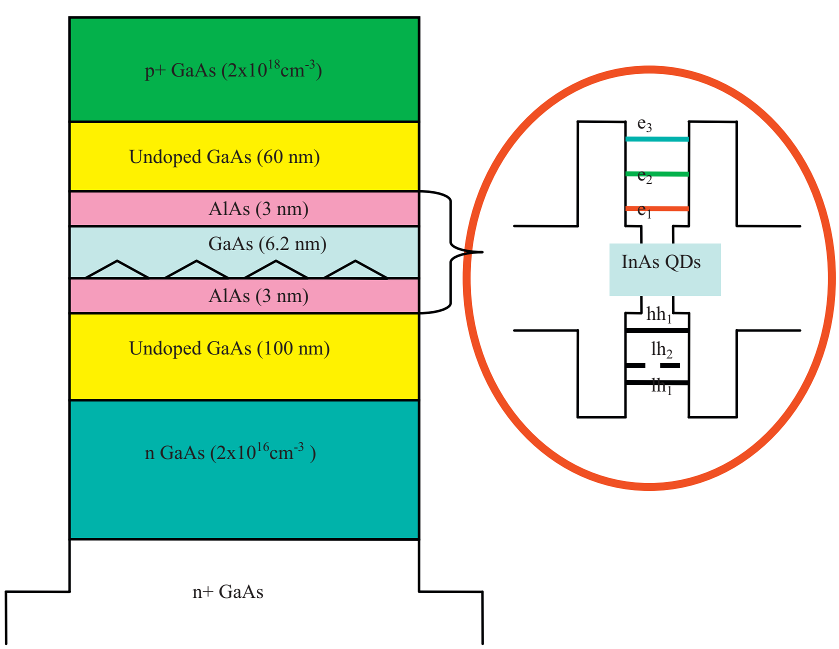

Figure 1 (online colour at: www.pss-a.com) Device structure and energy diagram in the intrinsic region (at zero-bias).

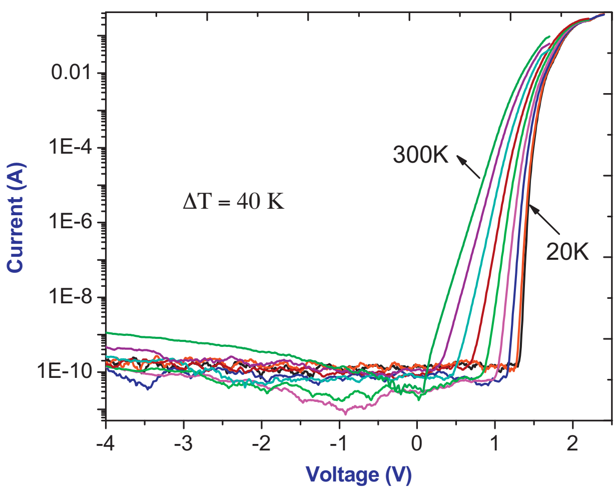

Figure 2 (online colour at: www.pss-a.com) Measured current–voltage characteristics at various temperatures.

The derived ideality factor from the I–V semi-logarithmic plot, depicted in Fig. 3 as a function of temperature, is practically unvarying above 140 K. However, the significant increase in n as the temperature is decreased below 120 K might be an indication that a different conduction process dominates over this lower temperature range.

To pursue this point further and gather additional information regarding these processes, the variations of n *versus* temperature are examined more closely in two temperature ranges. First, above 140 K the ideality factor (labeled, n_H, in the inset of Fig. 4) is nearly constant with only a slight dependence on temperature and it turns out that in this region n_H is best described by the equation:

$$\frac{1}{n_H} = \frac{1}{n_0} + \frac{T}{n_0 T^*}. \tag{2}$$

This corresponds to the situation of standard bulk recombination of electron–hole pairs via an exponential

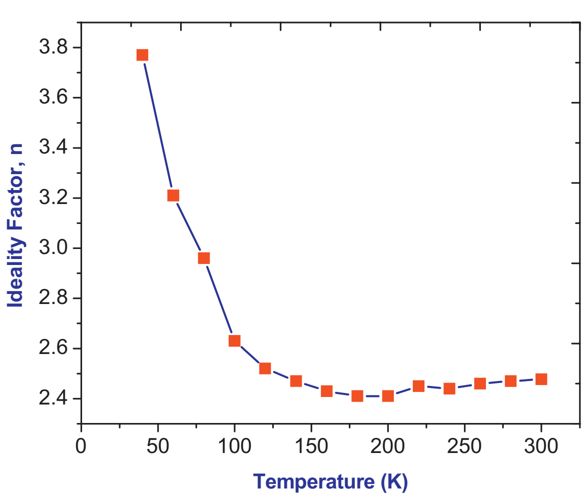

Figure 3 (online colour at: www.pss-a.com) Variations of the ideality factor with temperature.

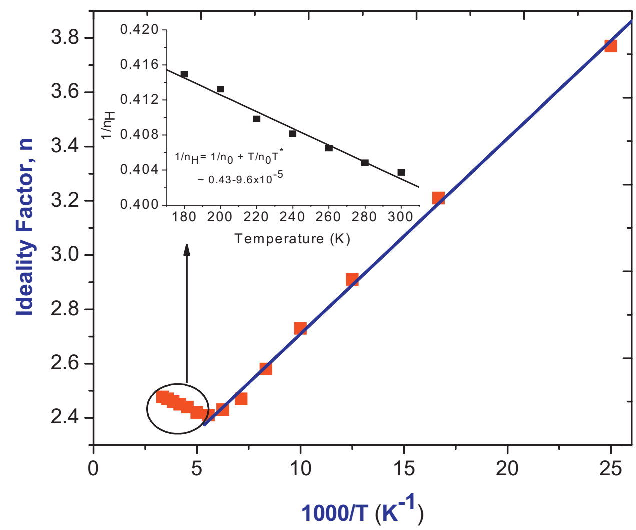

Figure 4 (online colour at: www.pss-a.com) The different trends of ideality factor over low and high temperature regions.

distribution of trap states [6]. Fitting the derived n_H to Eq. (2) yields a value of 2.3 for n_0 suggesting, indeed, that the conduction mechanism is likely taking place through mainly recombination. Alternatively, in the lower temperature region the ideality factor varies with $1/T$ (Fig. 4), so that the slope q/nkT, in Eq. (1) above, remains temperature independent and Eq. (1) can then be approximated by $I = I_s(T)e^{AV}$, where A is a temperature independent coefficient. This situation corresponds adequately to a conduction mechanism that is dominated by tunneling assisted by recombination via trap centers as proposed by Riben and Feucht [14, 15].

Analyzing the reverse bias regime, the dark current for the diodes is between 10^{-9} and 10^{-10} A at -2 V indicating that the devices are of good quality. This dark current should vary as:

$$I_s = I_0 \exp(-E/nkT), \tag{3}$$

where I_0 contains all the junction parameters such as diffusion coefficients, diffusion lengths, and doping levels while E is an activation energy that should be equal to the energy bandgap (E_g).

Considering the current variations with the inverse temperature above 100 K [Arrhenius plot, $\ln(I_s)$ *versus* $1/nT$, shown in Fig. 5], this shows an exponential decay in line with the above relation, where the extracted activation energy ($\sim$1.6 eV) is just a little higher than the fundamental E_g of GaAs. This is likely signifying that bulk rather than interface recombination dominates (the activation energy would have been closer to the built-in potential in case of interface recombination).

The fact that there is a change of regime from a temperature independent behavior (for temperatures below 100 K the dark current becomes independent of T) to an

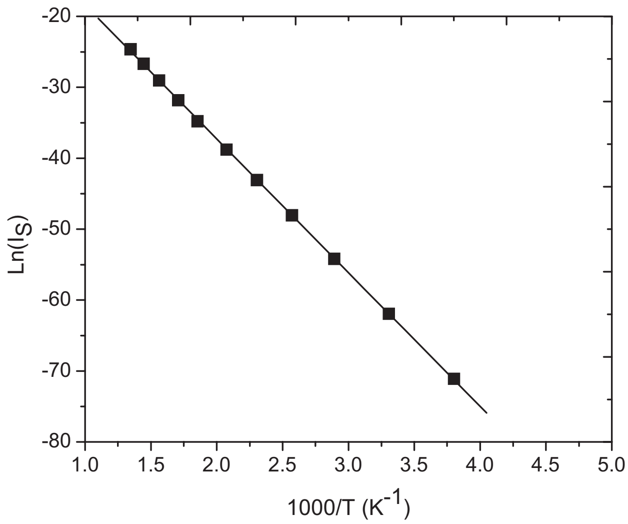

Figure 5 Variations of the saturation dark current as a function of temperature.

exponential increase with temperature can be explained by a possible detrapping of carriers at around 100 K.

Moreover, a negative differential resistance (NDR) region is clearly observed at 180 K (Fig. 6) and at temperatures below. The appearance of this NDR is due to resonant tunneling of electrons (holes) through the quasi-bound levels in the GaAs QW and also suggests that the current mechanism is directly related to the presence of quantum states in the well region and may be controlled by their net charge. Our interpretation below, in this respect, follows that of Kiesslich et al. [1], while noting that in the temperature range considered in our case – which is well above and complements that of Kiesslich et al., there is no observed resonance that corresponds to the quantum state e_1. The NDR region becomes more prominent at lower

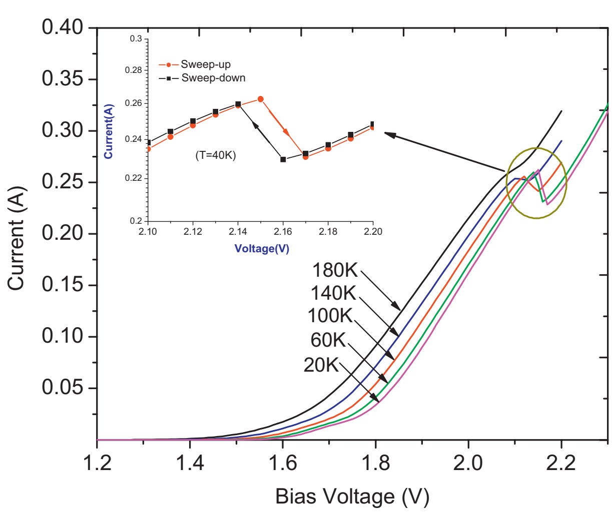

Figure 6 (online colour at: www.pss-a.com) Linear *I–V* characteristics showing NDR regions. The inset shows the Z-shaped bi-stability recorded in the NDR region.

temperatures with its voltage position being shifted to slightly higher values as the temperature is decreased. The peak-to-valley ratio and the peak current density noticeably increase, as expected, with decreasing temperature.

The temperature should have no influence on the tunneling process but the contribution of thermally activated processes diminishes considerably at low temperatures leading to more perceptible tunneling features.

The QW states were obtained through the numerical resolution of the one-dimensional time-independent Schrodinger equation with the use of effective mass approximation for the case of a rectangular AlAs/GaAs/AlAs single well double barrier structure having a well width of 6.2 nm and symmetric barriers 3 nm thick. The energy levels due to both light- and heavy-holes in the valence band have been taken into account in the calculations of the bound energy levels (or transitions). The electron (e), light hole (lh), and heavy hole (hh) effective masses in GaAs and AlAs as well as the band gaps, and hence the barrier discontinuity, were taken from Ref. [16]. Calculated transition energies between the lowest conduction band levels and highest valence band levels were obtained to be 1.56 eV for the transition e_1–hh_1, 1.62 eV for the transitions e_1–lh_1 and e_1–hh_2 and 1.94 eV for the transitions e_2–lh_1 and e_2–hh_2.

In order for resonant tunneling of electrons or/and holes to occur, the applied voltage must first exceed the flat-band value of the built-in voltage corresponding to the energy gap of GaAs ($E_g/e \sim 1.42$ eV), then an additional applied voltage is required so as to make the energy of tunneling electrons (holes) coincide with that of the quasi-bound state in the well (GaAs) region. Considering this, it appears that the NDR region observable in the linear-scale *I–V* characteristics of the p–i–n diodes under study relates to tunneling through the second energy state (e_2).

It is noteworthy mentioning that the light-hole effective mass in the GaAs QW is about 30% larger than that of conduction electrons implying that the light-hole energy level in the valence band should be lower than that of conduction electrons. It is predicted, however, that the applied voltage required for electron- and hole-resonances be approximately the same because the bound state energy of electrons in the electron-accumulation layer is larger than that of holes in the hole-accumulation layer [17].

Obviously, the NDR is much clearly perceptible when plotting the first derivative of the current (d*I*/d*V*). From these plots (Fig. 7) it can be also observed that another NDR region is present and this becomes progressively discernible as the temperature decreases. This NDR region is very likely due to resonant tunneling through the energy level lh_1 (hh_2). One can also note that, in the range of temperatures considered, there is no other evidence of effects due to the presence of QDs except a possible lowering of the electron quasi-energy levels in the well region.

Embedding InAs QDs in the GaAs well is known to affect the energy structure of the GaAs QW by shifting the energy states to lower values, which seem to be the case here, and which will explain the absence of an NDR due to e_1.

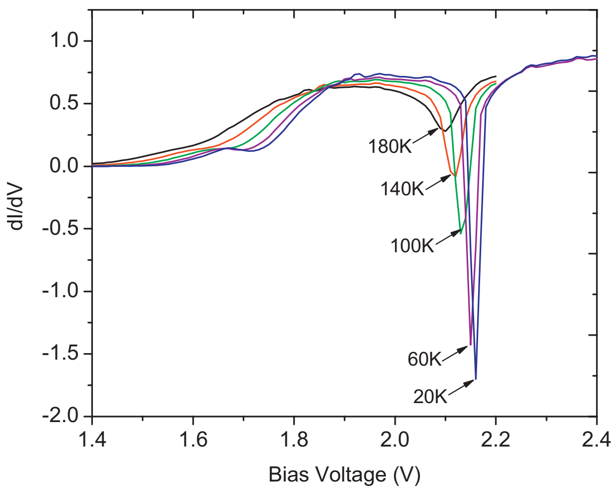

Figure 7 (online colour at: www.pss-a.com) First derivative of current showing clearly the NDR regions.

In fact, the QD layer and the wetting layer underneath affects in particular the even-parity states (such as e_1, hh_1, and lh_1) in the QW by lowering their energy values while leaving the odd-parity states (such as e_2) unaffected because of the antinode in its wave function at the center of the QW [18]. Pulizzi et al. [19], studied a similar resonant tunneling structure and attributed the absence of resonance due to e_1 to electrons being strongly scattered by the presence of disorder in the well region, leading to a condition of momentum non-conservation. They have been able, however, to compensate for the momentum loss due to disorder and recover the resonance peak due to e_1 by providing the electrons with additional momentum through the appropriate application of a magnetic field.

Furthermore, the Z-shaped bistability observed in the NDR region of the *I–V* characteristics at voltages beyond the flat band condition is persistent, in the lower range of temperatures considered here, when sweeping the bias in the opposite direction (inset of Fig. 6). Studying similar structures, Kiesslich et al. [1] have also observed an S-shaped hysterisis at $T = 30$ mK in the bias region below the flat band condition and have linked this to the presence of QDs and the different electron- and hole-injection rates in and out of the well region. This S-bistability seems, however, to have smeared out in the temperature range considered in our case. It is pertinent to note, in this context, that there are trends and features in structures containing QDs that have been observed and resolved through optically excited carriers (such as luminescence) but have not been possible to reproduce by electrically injected carriers [7].

4 Conclusions The measured dark current in p–i–n diodes, incorporating, in their intrinsic region, a GaAs QW sandwiched between two AlAs barriers, were analyzed in the temperature range 20–300 K. The analyses revealed that bulk recombination and tunneling assisted recombination govern the dark conduction in the bias region below the flat band condition. At higher applied forward voltages and at temperatures below 180 K, the current appears to be controlled by resonant tunneling through the energy states in the well region. In the temperature range considered, there is no evidence of effects due to the embedded QD layer apart from a possible lowering of the first (even-parity) energy state in the well.

Acknowledgements Z. O. would like to thank Sultan Qaboos University for hosting him during his sabbatical leave.

References

[1] G. Kiesslich, A. Wacker, E. Scholl, S. A. Vitusevich, A. E. Belayev, S. V. Danylyuk, A. Forster, N. Klein, and M. Henini, Phys. Rev. B **68**, 125331 (2003).
[2] K. W. J. Barnham and G. Duggan, J. Appl. Phys. **67**, 3490 (1990).
[3] K. W. J. Barnham, B. Braun, J. Nelson, and M. Paxman, Appl. Phys. Lett. **59**, 135 (1991).
[4] L. Ballard, J. Nelson, K. W. J. Barnham, J. Connolly, J. S. Roberts, and M. A. Pate, Proc. 2nd World Conference and Exhibition on Photovoltaic Solar Energy Conversion (Vienna, Austria, 1998), p. 227.
[5] A. E. Belayev, A. Patane, L. Eaves, P. C. Main, M. Henini, and S. V. Danylyuk, Nanotechnology **12**, 515 (2001).
[6] V. Nadenau, U. Rau, A. Jasenek, and H. W. Schock, J. Appl. Phys. **87**, 584 (2000).
[7] H. Buhmann, L. Mansouri, J. Wang, P. H. Beton, L. Eaves, and M. Henini, Appl. Phys. Lett. **65**, 3332 (1994).
[8] A. V. Sachenko and I. O. Sokolovskyi, Semicond. Phys., Quantum Electron. Optoelectron. **11**, 1 (2008).
[9] S. Huang, IEEE Trans. Nanotechnol. **9**, 142 (2010).
[10] A. Baumgartner, A. Chaggar, A. Patane, L. Eaves, and M. Henini, Appl. Phys. Lett. **92**, 091121 (2008).
[11] F. Renner, M. Eckardt, A. Schwanhausser, O. Klar, S. Maizer, G. H. Dohler, G. Loata, T. Loffler, H. Roskos, M. Hanson, D. Driscoll, and A. C. Gossard, Phys. Status Solidi A **202**, 965 (2005).
[12] A. L. Bavencove, G. Tourbot, E. Pougeoise, J. Garcia, P. Gilet, F. Levy, B. Andre, G. Feuillet, B. Gayral, B. Daudin, and Le Si Dang, Phys. Status Solidi A **207**, 1425 (2010).
[13] K. Miki, T. Abe, J. Naruse, K. Ikumi, T. Yamaguchi, H. Kasada, and K. Ando, Phys. Status Solidi B **243**, 950 (2006).
[14] A. R. Riben and D. L. Feucht, Solid State Electron. **9**, 1055 (1996).
[15] M. P. Pires, F. C. Guastavino, B. Yavich, P. L. Souza, A. E. Mwongbote, and M. Valenza, IEEE Trans. Electron. Dev. **52**, 1949 (2005).
[16] S. Adachi, Physical Properties of III–V Semiconductor Compounds (Wiley-Interscience Publications, New York, 1992).
[17] P. M. Martin, R. K. Hayden, C. R. H. White, M. Henini, L. Eaves, D. K. Maude, J. C. Portal, G. Hill, and M. A. Pate, Semicond. Sci. Technol. **7**, B456 (1992).
[18] A. Patanè, A. Polimeni, L. Eaves, P. C. Main, M. Henini, Yu. V. Dubrovskii, A. E. Belyaev, P. N. Brounkov, E. E. Vdovin, Yu. N. Khanin, and G. Hill, J. Appl. Phys. **88**, 2005 (2000).
[19] F. Pulizzi, E. E. Vdovin, K. Takehana, Yu. V. Dubrovskii, A. Patane, L. Eaves, M. Henini, P. N. Brunkov, and G. Hill, Phys. Rev. B **68**, 155315 (2003).